Available online at www.sciencedirect.com

ScienceDirect

Procedia Engineering 13 (2011) 265–270

Engineering Procedia

5th Asia-Pacific Congress on Sports Technology (APCST)

# Aerodynamic properties of an arrow: Influence of point shape on the boundary layer transition

K Mukaiyama[a*], K Suzuki[a], T Miyazaki[a], H Sawada[b]

[a]*University of Electro-Communications, Chofu, Tokyo 182-8585, Japan*
[b]*Tohoku University, Sendai, Miyagi 980-8577, Japan*

Received 16 March 2011; revised 9 May 2011; accepted 11 May 2011

**Abstract**

Using two high-speed video cameras, we recorded the trajectory of an arrow (archery and crossbow) and analyzed its velocity decay rate, from which we determined the drag coefficient. In order to investigate *Re* number dependence of the drag coefficient, we developed a new arrow-shooting system using compressed air as a power source, which enabled us to launch an arrow at an arbitrary velocity (up to 60m/sec). We attached three points of different type (streamlined, bullet and bluff bodied) to the arrow-nose. The boundary layer is laminar for the streamlined point and turbulent for other points, in the measured *Re*-range ($0.78\times10^6 < Re < 1.65\times10^6$). These results are consistent with those from support-free wind tunnel measurements using JAXA's 60cm Magnetic Suspension and Balance System (MSBS), confirming that the point-shape has a crucial effect on the laminar-turbulent transition of the boundary layer.


Selection and peer-review under responsibility of RMIT University
*Keywords*: Arrow ; drag coefficient ; boundary layer transition

## 1. Introduction

Bows and arrows have long history and were used in both hunting and warfare until the invention of the gunpowder musket. They have been highly refined and improved as sports equipment by modern technologies. In fact, the winner scores in archery tournaments have become higher and higher. There are, however, few scientific studies on the aerodynamics of an arrow. This is mainly because its motion in flight is very complicated. An arrow spins around its axis of revolution, as well as it oscillates along its

* Corresponding author. Tel.: +81-42-443-5390; fax: +81-42-488-6371.
*E-mail address*: mukaiyam@miyazaki.mce.uec.ac.jp.


doi:10.1016/j.proeng.2011.05.083

length. It is quite difficult to reproduce these complicated motions in wind tunnel experiments. Even if we ignore the oscillatory motion and consider an arrow as a thin rigid body, any kind of mechanical supporting system disturbs the flow field largely and makes the measurement of aerodynamic forces acting on it inaccurate [1].

In this paper, we propose two ideas realizing support-interference-free measurements. First, we perform flight-experiment, in which we record the trajectory of the arrow using two high-speed cameras. The drag coefficient is determined from the velocity decay rate. An arrow-shooting system using compressed air as a power source is developed. It can launch an arrow at an arbitrary speed up to 60m/sec. Second, the aerodynamic forces are measured in the wind tunnel with JAXA's 60-cm Magnetic Suspension and Balance System, in which the force supporting the arrow is generated by magnetic fields. In order to measure the aerodynamic drag, lift and pitching moment in a wider *Re*-range, we introduce a model, which is about twice larger, in addition to the real arrow. Three points (streamlined, bullet and bluff bodied) are attached to the arrow-nose and their influence on the aerodynamics is investigated.

**Nomenclature**

| | | | |
|---|---|---|---|
| $Re$ | Reynolds number | $\rho$, $\mu$ | density and viscosity of air |
| $r$, $l$ | radius and length of arrow shaft | $F_D$, $C_D$ | drag force and its coefficient |
| $F_L$, $C_L$ | lift force and its coefficient | $M$, $C_M$ | pitching moment and its coefficient |

## 2. Experiments

We investigate, as a first step, the aerodynamics of a crossbow arrow (bolt) which is shorter and stiffer than arrows used in archery, behaving as a rigid body in its flight. The rotation rate of a crossbow arrow (4 $sec^{-1}$) is much smaller than that of an archery arrow (about 60 $sec^{-1}$), having very weak effect on the aerodynamics.

### *2.1. Crossbow Arrow and Launching System*

We use a crossbow arrow (Horton Steelforce) with length 0.502m and weight 0.0211kg (without point). The radius of the shaft is 0.00439m (Figure 1). Three kinds of point are attached to its nose (Figures 2(a)-(c)). The bullet point and bluff bodied point are commercially provided, whereas the streamlined point is originally produced by filing the bluff bodied point. The weights of the arrow with these points are 0.0275kg (bullet), 0.0276kg (streamlined) and 0.0283kg (bluff-bodied), respectively.

Since a crossbow launches an arrow only at a fixed speed of its own, we developed an arrow-launcher which blows the arrow by compressed air (Figure 3). The speed can be increased arbitrary up to 60m/sec, by adjusting the air pressure up to 4.4MPa. Its accuracy is high enough to hit an apple 50m apart. The Reynolds number *Re* is defined using the length of the arrow $l$, the velocity $u$, the density of air $\rho$ and the viscosity $\mu$:

$$Re = \frac{lu\rho}{\mu} \qquad (1)$$

We investigate a *Re* number range ($0.78 \times 10^6 < Re < 1.65 \times 10^6$), (corresponding the speed range $25[m/s] < u < 49[m/s]$) in the flight experiment, whereas a wider *Re* number range ($0.29 \times 10^6 < Re < 2.92 \times 10^6$) is scanned in the wind tunnel experiments.

Fig. 1. Crossbow arrow (Horton Steelforce)

Fig. 2. Three points; (a) bullet (b) streamlined (c) bluff bodied

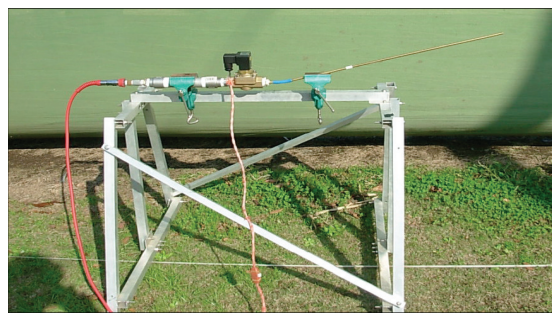

Fig. 3. Arrow launching system

### *2.2. Flight experiment*

Flight experiments are performed at the archery range of the Univ. Electro-communications. We use two high-speed video cameras (Phantom: Vision Research) with the spatial resolution of 512×256 pixels and the temporal resolution 2,000 fps. One camera is located at the place 5m apart from the launching machine and the other at the place 30m away from the first camera. They record the side views of the flying arrow (Figure 4). We analyze the video images to determine the horizontal and vertical velocity components of the arrow at these two locations, from which we can estimate the drag-coefficient $C_D$ assuming that no lift force is acting on the arrow, i.e., the arrow flies ideally with zero angle of attack (see Suzuki *et al.* [2] for the details of analysis).

### *2.3. Wind tunnel experiment*

The Magnetic Suspension and Balance System (MSBS) provides support-interference-free measurements, because the force supporting the arrow is generated by magnetic fields controlled by coils arranged outside the test section (Figure 5) [3]. We insert cylindrical permanent magnets inside the arrow shaft. The arrow is supported to be still against the gravitational and aerodynamic forces, by adjusting the electric currents. Then, we know inversely the aerodynamic forces acting on the arrow from the values of electric currents. The maximum speed (45m/sec) of the wind tunnel is less than the speed of the arrow launched from the crossbow (about 60m/sec). We use both the real arrow and a model which is 2.05 times larger, so that we can investigate a wider *Re* number range ($0.29 \times 10^6 < Re < 2.92 \times 10^6$) in our wind tunnel experiments.

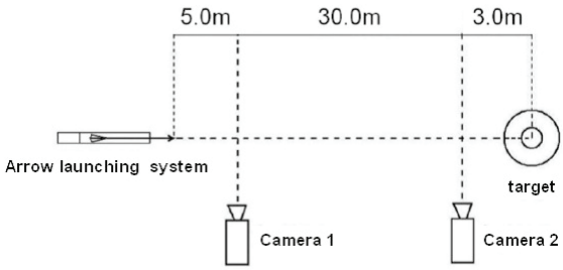


Fig. 4. Arrangements of experimental apparatus

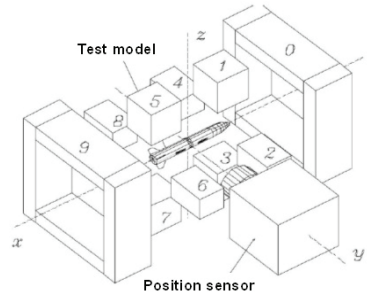


Fig. 5. Coil arrangements of MSBS (from Sawada and Kunimasu [3])

## 3. Results and Discussion

We present the results on the drag force. The drag force $F_D$ is non-dimensionalized in the form of the drag coefficient $C_D$ as,

$$F_D = \frac{1}{2} C_D \rho u^2 \pi r^2 \qquad (2)$$

Figures 6(a)-(c) illustrate the *Re* number dependence of $C_D$ for three points, i.e., (a) bullet, (b) streamlined and (c) bluff bodied, respectively. Symbols with error bars are from the flight experiment and the lines show the results of the wind tunnel measurements. The thicker broken lines are the results for the real arrow and the dotted lines are for the model. We can see that these two experiments provide generally consistent results. The values of $C_D$ for (a) bullet and (c) bluff bodied points are significantly larger than those for (b) streamlined point. This indicates that the boundary layer is turbulent for the former two cases and laminar for the last case. According to a linear instability theory under the parallel flow approximation, the laminar boundary layer formed on the arrow shaft is linearly stable against axisymmetric disturbances [4], in the investigated *Re* number range. Then the transition to turbulence is subcritical and induced by disturbances of finite amplitude introduced at the point, such as the breakdown of a separation bubble. If we look at Figure 6(a) in detail, we notice that the boundary layer transitions occur at different *Re* numbers for the real ($0.55 \times 10^6$) and model ($1.45 \times 10^6$) arrows. This is presumably because of the slight difference in the shape of the real and model points. Also, in Figure 6(c), $C_D$ of the model arrow is about 10% larger than $C_D$ of the real arrow for the same reason.

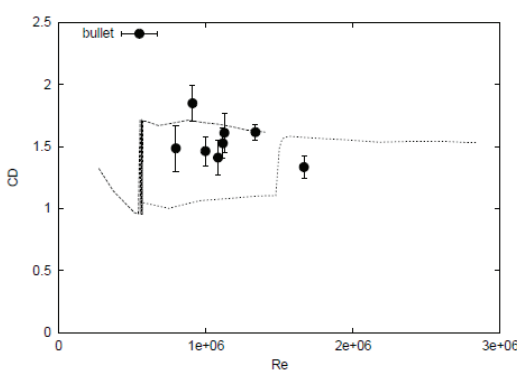


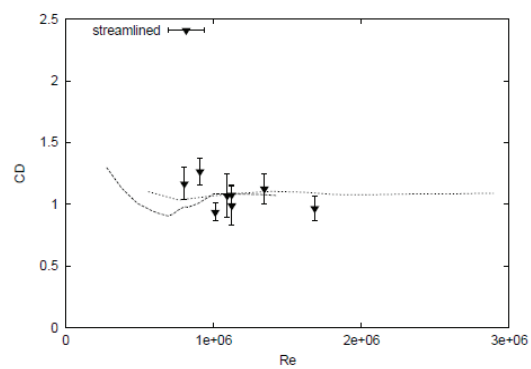

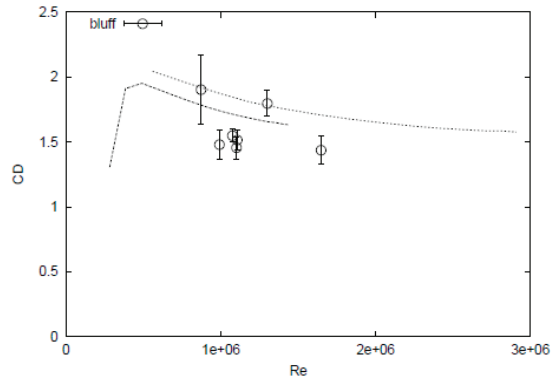


Fig. 6. Reynolds number dependence of $C_D$ (a) bullet point (b) streamlined point (c) bluff bodied point

We show, in Figure 7, the dependence of $C_D$ on the angle of attack $\psi$ of the real arrow. Closed triangles denote the results for the streamlined point at two *Re* numbers, where the boundary layer is laminar, whereas open circles show the results for the bluff bodied point, i.e., for turbulent boundary layer. We notice that $C_D$ increase gradually with the angle of attack $|\psi|$, if the boundary layer remains laminar, and $C_D$ remains almost constant when the boundary layer is turbulent. Closed circles illustrate the results for the bullet-point at three *Re* numbers near the laminar to turbulent transition of the boundary layer. We observe the abrupt increase of $C_D$ at certain small angles $|\psi|$, indicating that the transition to turbulent boundary layer is also induced by asymmetric disturbances of finite amplitude. This finding tells that even a small deviation from ideal flight with zero angle of attack will cause the subcritical transition of the boundary layer and the resulting increase of $C_D$, if the arrow speed is slightly less than the critical speed corresponding to the critical *Re* number.

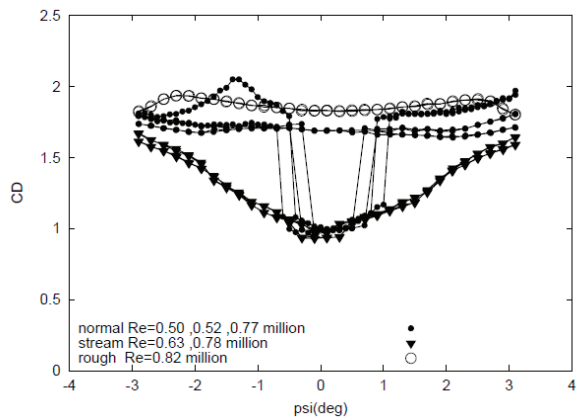


Fig.7. $C_D$ as a function of the angle of attack $\psi$

Finally, we illustrate the results on the lift force $F_L$ and the pitching moment $M$ acting on a real arrow in Figure 8 and Figure 9, respectively. These values are non-dimensionalized as follows:

$$F_L = \frac{1}{2} C_L \rho u^2 \pi r^2 , \quad M = \frac{1}{2} C_M \rho u^2 \pi r^2 l \qquad (3), (4)$$

They depend on the angle of attack $\psi$ linearly. The lift force increases with $\psi$, whereas the pitching moment decreases with $\psi$. The latter tells that the vane stabilizes the ideal arrow flight with zero angle of attack. The point-shape has little effect both on $C_L$ and $C_M$, probably because the lift force and the pitching moment are exerted on the vanes, mainly.

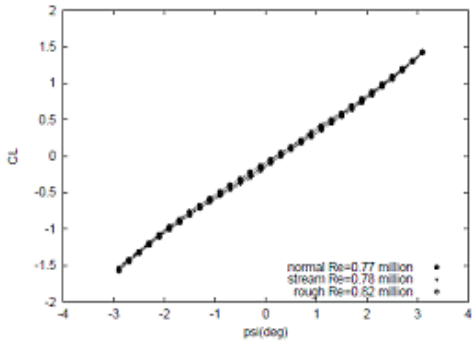


Fig. 8. $C_L$ as a function of $\psi$; $Re \fallingdotseq 0.8 \times 10^6$

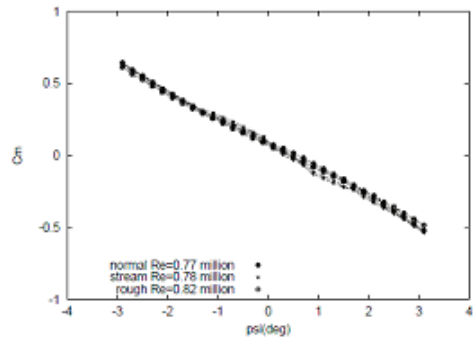


Fig. 9. $C_M$ as a function of $\psi$; $Re \fallingdotseq 0.8 \times 10^6$

## 4. Conclusion

We have investigated the aerodynamic forces acting on a crossbow arrow by the flight-experiment using two high-speed cameras and the wind tunnel experiment using JAXA's 60cm Magnetic Suspension and Balance System. The results from both experiments give a consistent picture and show that the point-shape has a crucial influence on the drag coefficient of an arrow. The boundary layer is laminar for the streamlined point and turbulent for bullet and bluff bodied points in the measured *Re* number range. The same experimental techniques make it possible to study the aerodynamics of archery arrows, such as A/C/E and X10 of Easton.

## Acknowledgements

This work is partially supported by a Grant-in-Aid (No. 19500557) from the Ministry of Education, Culture, Sports, Science and Technology. We wish to express our deep gratitude to Dr. Himeno for allowing us to use the high-speed video cameras. Without them, the flight experiment would have been impossible.

## References

[1]Sawada, H.: Experimental Study of Aerodynamic Performance of Arrows with JAXA's 60cm Magnetic Suspension and Balance System, Theoretical and Applied Mechanics Japan, Vol.56, 2007, pp.237-242

[2] Suzuki, K, Masui, K, Mukaiyama, K, Miyazaki, T. and Sawada, H.: Aerodynamic Properties of an Arrow – Influence of Point-shape on the Boundary Layer Transition -, Nagare, Vol.29 (4), 2010, pp.287-296 (in Japanese)

[3] Sawada, H and Kunimasu, T.: Development of a 60 cm magnetic suspension system for low-velocity wind tunnels. JJSASS Vol. 50(580), 2002, pp.188-195

[4] Tutty, O.R., Price, W.G. and Parsons, A.T.: Boundary layer flow on a long thin cylinder, Phys. Fluids, Vol.14 (2), 2002, pp.628-637